SlLAX1 is Required for Normal Leaf Development Mediated by Balanced Adaxial and Abaxial Pavement Cell Growth in Tomato

Title

SlLAX1 is Required for Normal Leaf Development Mediated by Balanced Adaxial and Abaxial Pavement Cell Growth in Tomato

Running head (short title)

SlLAX1 is required for normal leaf development in tomato

Corresponding author

Prof. H. Ezura

Faculty of Life and Environmental Science, University of Tsukuba, Tsukuba, Ibaraki, 305-8577 Japan

E-mail: ezura.hiroshi.fa@u.tsukuba.ac.jp; Phone, +81-29-853-7263

Subject areas

(1) Growth and development

Number of black and white figures: 3

Number of colour figures: 5

Number of tables: 6

Type and number of supplementary material: 1 PDF file

Title

SlLAX1 is Required for Normal Leaf Development Mediated by Balanced Adaxial and Abaxial Pavement Cell Growth in Tomato

Running head (short title)

SlLAX1 is required for normal leaf development in tomato

Author list

Sri I. Pulungan[1], Ryoichi Yano[2], Yoshihiro Okabe[2,3], Takuji Ichino[2], Mikiko Kojima[4], Yumiko Takebayashi[4], Hitoshi Sakakibara[4], Tohru Ariizumi[2,3], Hiroshi Ezura[2,3*]

[1]Graduate School of Life and Environmental Sciences, University of Tsukuba, Tsukuba, Ibaraki, 305-8577 Japan

[2]Faculty of Life and Environmental Sciences, University of Tsukuba, Tsukuba, Ibaraki, 305-8577 Japan

[3]Tsukuba Plant Innovation Research Center, University of Tsukuba, Tsukuba, Ibaraki, 305-8577 Japan

[4]RIKEN Center for Sustainable Resource Science, 1-7-22, Suehiro, Tsurumi, Yokohama 230-0045, Japan

Corresponding author

Prof. H. Ezura

Faculty of Life and Environmental Science, University of Tsukuba, Tsukuba, Ibaraki, 305-8577 Japan

E-mail: ezura.hiroshi.fa@u.tsukuba.ac.jp; Phone, +81-29-853-7263

Abbreviations: a.a., amino acid; *curl,* curly leaf; EMS, ethyl methanesulfonate; IAA, indole-3- acetic acid; LAX, like AUX1; NBRP, National BioResources Project; NGS, next-generation sequencing; PAT, polar auxin transport; PM, plasma membrane; qRT-PCR, quantitative real time-PCR; SEM, scanning electron microscope; TILLING, Targeting Induced Local Lesions IN Genome; ES, exome sequence; WT, wild-type.

Abstract

Leaves are the major plant organs with a primary function for photosynthesis. Auxin controls various aspects of plant growth and development, including leaf initiation, expansion, and differentiation. Unique and intriguing auxin features include its polar transport, which is mainly controlled by the *AUX1/LAX* and *PIN* gene families as influx and efflux carriers, respectively. The role of *AUX1/ LAX* genes in root development is well documented, but the role of these genes in leaf morphogenesis remains unclear. Moreover, most studies have been conducted in the plant model *Arabidopsis thaliana*, while studies in tomato are still scarce. In this study, we isolated six lines of the allelic curly leaf phenotype '*curl*' mutants from a γ-ray and EMS (ethyl methanesulfonate) mutagenized population. Using a map-based cloning strategy combined with exome sequencing, we observed that a mutation is occurred in the *SlLAX1* gene (*Solyc09g014380*)), which is homologous to an *Arabidopsis* auxin influx carrier gene, *AUX1* (*AtAUX1*). Characterization of six alleles of single *curl* mutants revealed the pivotal role of *SlLAX1* in controlling tomato leaf flatness by balancing adaxial and abaxial pavement cell growth, which has not been reported in tomato. Using TILLING (Targeting Induced Local Lesions IN Genome) technology, we isolated an additional mutant allele of *SlLAX1* gene and this mutant showed a curled leaf phenotype similar to other *curl* mutants, suggesting that *Solyc09g014380* is responsible for the *curl* phenotype. These results showed that *SlLAX1* is required for normal leaf development mediated by balanced adaxial and abaxial pavement cell growth in tomato.

Keywords: auxin, c*url* mutants, curly leaf, *SlLAX1*, tomato

Introduction

Leaves are the major plant organs whose primary function involves photosynthesis. Leaves play a major role in sensing the quality, quantity and duration of light, all of which are crucial for complete plant growth and development. Understanding leaf initiation and development are important subjects in plant biology. Most leaves are dorsoventrally (upper to bottom) flattened and develop distinct upper (adaxial) and lower (abaxial) surfaces. Balanced coordination of polarity, auxin response, and cell division is essential for formation of normal and flat leaves development. Any imbalance of these coordination results in altered leaf shapes such as curly, crinkly, twisted, rolled, radial, or shrunken leaves (Yu et al. 2005, Liu et al. 2010, Liu et al. 2011, and Serrano-Cartagena et al. 1999). The formation of flat leaves enables the optimum capture of sunlight during photosynthesis.

An important factor controlling leaf morphogenesis is the phytohormone auxin. Indole-3-acetic acid (IAA) is the natural form of auxin that controls various aspects plant growth and development, including cell division, expansion and differentiation, leaf initiation, and morphogenesis. One of the unique and intriguing features of auxin is its transport (Paciorek et al. 2005, Tromas and Perrot-Rechenmann 2010). It is known that auxin is synthesized in young leaves and in the shoot apex and is transported basipetally to all plant organs (reviewed in Bennet et al. 1998, Tromas and Perrot-Rechenmann 2010). Auxin transport involves two patterns: long-distance transport through phloem and short-distance or cell-to-cell transport called polar auxin transport (PAT). At the cellular level, IAA is distributed through a combination of membrane diffusion (passive uptake), carrier-mediated uptake or proton-driven distribution (Delbarre et al. 1996). PAT contributes to 85% of short-distance auxin transport. It is well established that polar auxin localization controls the direction of auxin movement in whole-plant organs.

Several auxin carriers have been identified, including AUX1/LAX (LAX: like AUX1), PIN (*PIN*-FORMED) and PGP/MDR (P-glycoprotein/ multidrug resistance)-like proteins. AUX1/LAX is reported to be an auxin influx carrier that facilitates auxin movement from outside the cell to inside the cell, while PIN is an efflux carrier that pumps auxin from the cell into the intercellular space. PGP/MDR-like proteins are reported to have the ability to be either influx or efflux carriers (Yang and Murphy 2009), but the contribution of these proteins is considerably small compared to that of the AUX1/LAX and PIN families (Kramer and Bennet 2006, reviewed in Swarup and Peret 2012).

There are numerous studies highlighting the effects of mutations in *AUX/LAX* gene family in the model plant *Arabidopsis*. However, most studies have focused on root phenotypes. For instance, the AUX1/LAX family has

been reported to promote lateral root emergence and formation (Marchant et al. 2002, Swarup et al. 2008, reviewed in Peret et al. 2009), root gravitropism (Bennet et al. 1996, Marchant et al. 1999), and root-pathogen interactions (Lee et al. 2011). Recently, *AUX1* function in the aerial parts of plants has received interest, but studies are still considerably scarce. In *Arabidopsis*, *AUX1* has been reported to control phyllotaxis patterning (Bainbridge et al. 2008), vascular patterning, xylem differentiation (Fabregas et al. 2015), and leaf serration (Kasprzewska et al. 2015). Additionally, although PAT is governed and maintained by the coordinated action of AUX1/LAX and PIN carrier proteins, among auxin carriers, PIN1 is the most studied. The role of the PIN protein family in leaf morphogenesis is well documented, yet the role of AUX1/LAX remains neglected or is underestimated. Furthermore, almost all studies have been carried out in the model plant *Arabidopsis*, while the role of auxin influx carriers in other model plants such as tomato is poorly understood.

In this study, we isolated six lines of *curly leaf* (*curl*) mutants from the 'Micro-Tom' mutant population that had been previously established by γ-ray irradiation and EMS (ethyl methanesulfonate) treatment (Saito et al. 2011, Shikata et al. 2016). The *curl* mutants showed dorsoventrally impaired leaf flatness, which exhibited severe upward bending or hyponasty on the transverse axis. Through map-based cloning combined with exome sequencing (ES), we characterized six alleles of the curly leaf mutants, which have nonsense mutation in the *SlLAX1* gene. We reported that the *SlLAX1* gene controls curly leaf phenotype in the tomato *curl* mutants. This feature has never been characterized. The characterization of several alleles of single *curl* mutants in this study sheds light on the pivotal role of *SlLAX1* in controlling leaf flatness mediated by normal adaxial-abaxial pavement cell growth. We also combined forward and reverse genetic approaches to validate the candidate gene. Using TILLING technology, we screened another nonsense mutant allele that consistently shows a similar curly leaf phenotype with that of the *curl* mutants obtained by a forward genetic approach.

Result

Isolation and phenotypic characterization of the curly leaf mutants

We previously developed a large mutant population of 'Micro-Tom', a model tomato cultivar, using γ-ray irradiation and EMS mutagenesis (Saito et al. 2011, Shikata et al. 2016). Currently, we have 9,216 EMS mutant lines. From the M_3 generation of this mutant population, we isolated six mutant lines exhibiting a severe upward curly leaf (hyponastic) phenotype, three lines were used for further analysis (Fig. 1A, B). The newly developed young leaves of the *curl* mutants were flat and indistinguishable from those of wild-type (WT) (Fig. 1C, D), suggesting that the impairment of leaf curvature was not detectable at the early vegetative stage. The leaves

became curly about one month after sowing and were continuously curly until the end of growing period. The initiation of curly leaves was not related to the transition from the vegetative to the reproductive stage, and the leaf phenotype could not be restored at any stage once the curly leaves had formed. Growing the *curl* mutants in a high-humidity environment in *in vitro* culture could not rescue the curly phenotype (Fig 1E). Additionally, curly leaves continuously appeared irrespective of water availability in the soil medium (Fig. 1F, G). The leaf water potential of the mutants and WT was also comparable (Supplementary Table S1). These data suggested that the curly leaf mutant phenotype is persistent, irrespective of relative humidity or water availability.

We also analyzed the percentage of reduced leaf area and perimeter both in young and mature leaves of mutants by flattening the *curl* mutant leaves. In the young leaves, leaf area was markedly reduced (41.0 - 56.0%, Table 1). The leaf perimeters of the WT and mutants were comparable. Consistently, in the mature leaves, the reduction in leaf area was more evident (55.8 – 64.0%) (Table 1), indicating a progression of severity that was concomitant with leaf maturity. Then, to investigate how and when the curly leaf is formed and its progression at the organ level, we measured the curvature index (CI) in both young and mature leaves according to the method of Liu et al. (2010). Negative curvature represents upward bending of the leaf. At the early stage of leaf initiation and development, mutants developed and maintained flat leaves; after several (4-7) days following leaf initiation, the leaves gradually became curly, and the curly leaf severity increased concomitant leaf maturity (Supplementary Fig. S1A-C). The leaf incurvature was initiated from young leaves firstly at the tip along the transversal axis to a low extent, while the longitudinal axis remained flat in all mutant lines (Table 2, Fig. 2A, B). To understand the curly leaf progression, the global curvature of mature leaves of all mutants was also measured (Table 2). Consistently, leaf incurvature was observed along the transversal axis to a high extent and the longitudinal axis remained normal at all stages of leaf development. In the mature leaves, the whole-leaf had become curly (Fig. 2C, D). These data suggested that leaf incurvature was more severe as leaf maturity progressed.

Genetic mapping of *curl* mutants

To examine the inheritance pattern of the *curl* mutants, we crossed the mutants with the WT 'Micro-Tom' and another tomato cultivar 'Ailsa Craig', and observed the segregation ratio in the F_2 population. Phenotypic observation was carried out visually according to the presence or absence of the curly leaf phenotype. The mutant phenotype appeared in the F_2 generation only as a recessive genetic trait (Table 3). The ratio of WT and mutant phenotypes fit to Mendelian segregation ratio for monogenic traits (3:1), indicating a monogenic

recessive inheritance of all *curl* mutants. Similarly, in the 'Ailsa Craig' background, the inheritance of the *curl* mutants was also recessive (Supplementary Table S2). Allelism test was performed to observe complementation effects among mutant lines and to examine whether mutations occurred because of the same causal gene. The complementation effect was determined in the F_1 generation. All crosses between each pair of mutant lines showed curly leaf phenotypes (Table 4), indicating that they are allelic which means causal mutation occurred in the same locus. The *curl-6* mutant generated from EMS treatment (see Plant Material) was also allelic with the other mutants which were generated from γ-ray irradiation. We confirmed that all *curl* mutant lines were allelic, therefore, for further analyses we used only three mutant alleles, namely, *curl-1*, *curl-2*, and *curl-6*.

To identify the candidate gene controlling the curly leaf phenotype, we performed a map-based cloning approach using PCR-based DNA markers including CAPS and SNPs (Shirasawa et al. 2010, Chusreeaeom et al. 2014, Ariizumi et al. 2014, Hao et al. 2017). We found that the mutation likely occurred in the short arm of chromosome 9 (Supplementary Table S3). The highest 'Micro-Tom' allele frequency was observed in this chromosome region between markers tomInf5375 and 14109_151 and ranged from 0.68-0.89, suggesting that the responsible gene could be localized in the short arm of chromosome 9 close to marker 14109_151 (physical position SL2.40ch09: 2052389, Fig. 3).

SlAUX1 gene is commonly mutated in several _curl_ mutant alleles

To narrow down the candidate region obtained by rough mapping, we performed exome sequence (ES). Four lines of the *curl* mutants, *curl-1, curl-2, curl-3* and *curl-6* were used for the ES analysis. The F_2 progenies derived from the cross between mutant and WT 'Micro-Tom' were divided into flat leaf and curly phenotype based on presence or absence of curly leaf phenotype, and then flat leaf and mutant bulked segregants were subjected to exome sequencing. By bowtie2-GATK pipeline using the tomato genome reference version SL2.50 as a reference (see Materials and Methods), we identified 5,430, 5,110, 5,050, and 4,829 genome-wide mutations for *curl-1*, *curl-2*, *curl-3*, and *curl-6* mutant segregants, respectively. When allele frequencies were compared between these mutants, a strong association was found around the top region of chromosome 9 in all of the four mapping populations (Fig. 4). This result suggested that the causal gene for curly phenotype is located in this chromosome region, in agreement with the result of rough mapping of chromosome (Fig. 3, Supplementary Table S3). Furthermore, we then searched for the gene in which mutation is commonly occurring in some of the *curl* mutants. We found that mutations are commonly occurring in *Solyc09g014380.2.1*, which is a homologue of *Arabidopsis AtAUX1* (AT2G38120; BLASTx E-value = 0.0, protein amino acid similarity = 93%).

Solyc09g014380.2.1, tomato locus *SlLAX1,* gene spans ~3.8 kb genomic region, while cDNA including untranslated region (UTR) spans 1.8 kb. The *SlLAX1* has seven exons, including UTR region in both 5' and 3' ends (Fig. 4). The *curl*-2 and *curl*-6 had nucleotide substitution from G to A in the exon 6, physical position SL2.50ch09: 6010739 bp (Table 5). This SNP produced a premature stop codon (W262*) in the deduced protein sequence of SlLAX1. According to the SL2.50 tomato genome reference, WT 'Micro-Tom' produced 411 a.a. length of SlLAX1 protein, whereas the *curl-2* and *curl-6* mutants produced only 261 a.a. length of the protein., losing the last 150 a.a. (63.7% out of WT protein). *curl-1* and *curl-3* had SNP from G to T in the splicing junction of intron 4, physical position SL2.50ch09: 6009292 bp. These mutations were also confirmed by dideoxy sequencing of cDNA (Fig. 5A, B).

As described above, the *curl-1* and *curl*-3 had a mutation in the 1st nucleotide or splicing junction of intron 4 (Fig 4, Table 5). Interestingly, sequencing of *SlLAX1* cDNA in these alleles revealed that abnormal splicing is occurred around the intron 4, which led to deletion of five nucleotides within exon 4 (nucleic acid 433-437, Fig. 5C). Given that mutation in the *curl-1* and *curl-3* is G to T substitution in the splicing junction of intron 4, presumably, there was an alteration in donor and recipient sites for intron splicing. Splicing of intron 4 was occurred in the position of 435 bp from start codon in the tomato genome of the WT, whereas intron splicing is occurred in 5 bp upstream of the end of exon 4 (430 bp from start codon) in both the *curl-1* and the *curl-3* alleles. Then the next sequence from following exon 5 is GGTTGA; this TGA may produce premature stop codon, which is a position of 435 bp from the start codon (Fig. 5E). Thus, *curl-1* and *curl-3* alleles could produce a C-terminal truncated SlLAX1 protein that is only 145 a.a. length of protein (Fig. 5D). We also analyzed the transcript level of the *SlLAX1* by qRT-PCR using mature curly leaf cDNA. The expression of the *SlLAX1* gene in the three curly leaf mutants was significantly reduced to only 35-40% of WT expression (Fig. 5F), which indicates low abundance of this gene transcript in the mutants. Taken together, these results indicated that all of *curl* mutants carried loss-of-function mutation in the *SlLAX1* gene.

Screening a new allele of the nonsense mutation of *SlLAX1* by TILLING

Because our research group had previously developed large mutant resources in the 'Micro-Tom' background and proved that TILLING is an efficient tool for isolating desired mutants from the 'Micro-Tom' mutant collection (Okabe et al. 2011), we utilized TILLING to search for other *SlLAX1* mutant alleles. We screened 4,608 lines in the M_2 and M_3 generations to obtain new *SlLAX1* mutant alleles. In addition, because we only had one EMS mutant screened by forward genetics (*curl-6*), we attempted to obtain other mutant alleles to confirm

the phenotype consistency.

We designed a primer pair to amplify 865 bp along exon 6 of the *SlLAX1* gene for the TILLING screening target and found five new mutant alleles that carried intron, missense, and nonsense mutations (Supplementary Fig. S2A, B, Supplementary Table S5). The *curl-6*/TOMJPE8506, which was previously isolated by forward genetics, was also confirmed by TILLING screening. Then, to validate the mutant phenotype, one line that carried a nonsense mutation, TOMJPW601-1, was renamed as '*curl-7*' and used for further analysis. This mutant line carried a one base pair substitution from G to A in 554th nucleotide from start codon, which led to the conversion of tryptophan to a premature stop codon at the position of 185th a.a. (Fig. 6A). The *curl-7* mutant exhibited curly leaf phenotype like as the other *curl* mutant alleles (Fig. 6B). Furthermore, by dideoxy sequencing, we confirmed the consistency of the TILLING result (Fig. 6C, D). This result supports the evidence that *SlLAX1* is the gene responsible for the curly leaf phenotype in tomato. These results again indicated that mutation in *SlLAX1* produces the curly leaf phenotype. The mutations in the same gene consistently resulted the same phenotype, strongly suggesting that *SlLAX1* functions in controlling tomato curly leaf phenotype.

Endogenous IAA levels and the expression of auxin-related genes in *curl* mutants

As described above, all *curl* mutants commonly have mutation in the *SlLAX1* gene, which encodes an auxin influx carrier. To test the potential function of SlLAX1 as an auxin transporter in tomato, we measured the leaf auxin content at three stages: (i) in young leaves, (ii) before curly leaves formed when leaves just turned into curly; and (iii) in mature leaves, after leaves were fully curly. The IAA content significantly decreased from young leaves to mature leaves in both the WT and three *curl* mutants (Supplementary Fig. S3A). However, the IAA content at each leaf stage was comparable between the WT and the *curl* mutants. Similarly, IAA conjugates and total IAA between the WT and the *curl* mutants were also comparable (Supplementary Fig. S3B, C).

In *Arabidopsis*, numerous findings have indicated the role of LAX1/AUX1 family in root gravitropism and lateral root formation (Bennet et al. 1996, Marchant et al. 2002, reviewed in Swarup and Peret, 2012). Importantly, root agravitropism is the most prominent defect and well-characterized trait of the *Arabidopsis aux1* mutant. In addition, the *aux1* mutant also showed lateral root formation defects (Marchant et al. 2002). Thus, we further tested these traits in the *curl* mutants; as expected, the *curl* mutants showed agravitropism as well as reduced lateral root formation, in agreement with *Arabidopsis aux1* mutant phenotype (Supplementary Fig. S4), suggesting the possibility of involvement of SlLAX1 as an auxin influx carrier in tomato similar to AtAUX1.

Abaxial pavement cell size of the *curl* mutants were significantly larger

Because *SlLAX1* gene function was commonly disabled in *curl* mutants and auxin has been known to affect pavement cell (Pérez-Pérez et al. 2010, reviewed in Sandalio et al. 2016), we hypothesized that the curly leaf formation may related to differential cell growth on adaxial and abaxial surfaces. To observe histological features of the *curl* mutants, we measured pavement cell size using a scanning electron microscope (SEM) in the adaxial and abaxial surfaces at the mature leaf stage at the curly part (Table 6, Fig. 7). We noted that cell enlargement in the *curl* mutants was more prominent in the abaxial side, while there was no significant difference in adaxial pavement cell. As a consequence, the ratio of abaxial and adaxial pavement cell was more prominent in the *curl* mutants. We also quantified the pavement cell number both in adaxial and abaxial surfaces. The number of pavement cells in both surfaces was comparable (Table 6). These data revealed that the leaf flatness impairment of the *curl* mutants is likely due to the differential cell growth between the adaxial and abaxial epidermal layers. Most likely, the curly leaf phenotype is related to cell enlargement in abaxial side.

Relative expression of auxin-related genes in the *curl* mutants

Recently, some studies have reported that impairment auxin biosynthesis, signaling, degradation, and conjugation result in leaf development defect such as wrinkled, curled leaf, and rounded leaf phenotype. We checked relative expression of some putative tomato auxin-related genes which were reported involved to control leaf flatness phenotype such as *AtDof5.1* (Kim et al. 2010) which is homologous to *SlDof25* and *SlDof28* in tomato (Cai et al. 2013), *LCR* (*LEAF CURLING RESPONSIVENESS*) (Song et al. 2012), *PNH* (*PINHEAD*) (Newman et al. 2012), *YUC1* (Cheng et al. 2007). At the young leaf stage, the expression level of LCR gene was slightly decreased in the *curl* mutants compared to that of WT but increased in the mature leaf (Fig. 8C, I). *YUC1* expression was also significantly decreased both in the young and mature leaves of the *curl* mutants (Fig. 8D, J) There was no significant different in *Sldof28,* and *PNH* at both stages (Fig. 8B, H, E, K). *SlDof25* expression level was increased in the *curl* mutants at the mature leaf stage (Fig. 8G), while there was no significant change at the young leaf stage (Fig. 8A). It has been reported that *Arabidopsis* activation tagging mutant *Dof5.1-D* exhibited an upward-curling leaf phenotype by promoting *Revoluta* transcription (Kim et al. 2010). *Revoluta* (*Rev*) is an adaxial specification gene (Emery et al. 2003, Prigge et al. 2015). And most importantly, in tomato, it has also been reported that overexpression of a microRNA166-resistant version of *SLREV* (35S::REV^{Ris}) showed upward curly leaf phenotype (Hu et al. 2014). The gene expression of *SlDof 25* and *SlRev* was consistent with these findings (Fig. 8G, L).

Discussion

SlLAX1 gene is responsible for the curly leaf phenotype in tomato

We characterized several alleles of tomato mutants exhibiting severe upward-curling leaf phenotypes at the mature leaf stage (Fig. 1A, B). This mutant phenotype occurred irrespective of water content or relative humidity (Fig. 1E, G, Supplementary Table S1). Six lines were isolated using a forward genetic approach by visually selecting curly leaf phenotypes in a previously generated tomato mutant population (Saito et al. 2011, Shikata et al. 2016).

Map-based cloning combined with ES revealed that the mutation occurred in the *SlLAX1* (*Solyc09g014380*) gene (Fig. 3, 4). Then, to validate the candidate gene, we utilized TILLING to obtain additional allelic line with nonsense mutation, *curl-7*, which was generated by EMS. The *curl-7* mutant leaves displayed similar curly leaves to the other *curl* mutants (Fig. 6B). Furthermore, we confirmed the full-length coding sequence of *SlLAX1* (Fig. 6C, D), which supported the evidence that *SlLAX1* is the gene responsible for the curly leaf phenotype. Taken together, the characterization of multiple alleles in this study that consistently showed similar phenotypes is strong evidence for the role of *SlLAX1* in controlling the curly leaf phenotype. To our knowledge, this study is the first example of the successful exome sequence application in tomato in the identification of causal gene preceded by a forward genetic approach.

SlLAX1 encodes a transmembrane amino acid transporter protein and belongs to the amino acid/auxin permease (AAAP) family. Homology searches indicated that the SlLAX1 protein sequence is homologous to *Arabidopsis thaliana AtAUX1* (AT2G38120). In *Arabidopsis*, AUX1 is one of four auxin influx carriers belonging to AUX1/LAX family that controls several developmental processes including gravitropism responses, venation patterns, and lateral roots (Vieten et al. 2007, Bennet et al. 1996). Although recent findings have indicated that the AUX/LAX1 family also control aerial part development such as leaf serration (Kasprzewska et al. 2015), phyllotaxis patterning, vascular patterning, and xylem differentiation (Bainbridge et al. 2008, Fabregas et al. 2015), the role of AUX1/LAX gene family in leaf curling are poorly understood. In contrast, mutations in many auxin-related genes showed an impaired leaf flatness phenotype (Esteve-Bruna et al. 2013, Zgurski et al. 2005). In tomato, few studies have shown a relationship between auxin and leaf flatness; for instance, *SlARF4-RNAi* lines produce hyponastic leaves (Sagar et al. 2013) and *SlPIN4-RNAi* lines show leaf flatness defects as well as altered plant architecture (Pattison and Catala 2012). However, the role of *SlLAX1* in controlling leaf curly phenotype has not been reported in tomato or other major crops.

The tomato *AUX1/LAX* family consists of five genes (*SlLAX1-5*). They share high identity and similarity; the

identity of *SlLAX2*, *SlLAX3*, *SlLAX4*, and *SlLAX5* with *SlLAX1* are 80.36%, 79.70%, 92.65%, and 80.87%, respectively (Sol Genomics Network). All *SlLAX* genes are expressed in the mature leave and root of tomato (Pattison and Catala 2012). The single mutants depleting *SlLAX1* used in this study, *curl-1-7,* showed a severe phenotype effect in leaf flatness, suggesting that the importance of *SlLAX1* in controlling leaf flatness in mature leaves. Although the functional redundancy of the *AUX1/LAX* family, in addition to the function of *SlLAX1* itself, is poorly characterized in tomato, their function in *Arabidopsis* is well characterized especially in root development. Although four *AUX1/LAX* genes share high sequence identity and similarity, *AtAUX1* has the strongest auxin influx activity (Peret et al. 2012, Rutschow et al. 2014). Peret et al. (2012) also reported that subfunctionalization of the AUX1/LAX family in root based on their distinct pattern of spatial expression and the subcellular localization. In contrast, the *AUX1/LAX* genes play redundantly in the context of phyllotaxy, vascular patterning, and xylem differentiation (Bainbridge et al. 2008, Fabregas et al. 2015). Therefore, the functional redundancy of *SlLAXs* family in tomato leaf curling phenotype awaits further investigation.

Loss-of-function of SlLAX1 protein is related to the curly leaf phenotype

Based on experimental evidence, Swarup et al. (2004) reported that *Arabidopsis* AUX1 protein has eleven transmembrane (TM) helixes. Using publicly available server, we checked the prediction of transmembrane helices in the SlLAX1 protein. According to a prediction program in http://www.cbs.dtu.dk/services/TMHMM/, both AtAUX1 and SlLAX1 (Supplementary Fig. S5A) have 10 TM helixes. The *curl-2* and *curl-6* mutants (Fig. 5B) carry a nonsense mutation which is located in the TM helix VII (Supplementary Fig. S5C) according to TMHMM, which is equivalent to the central region of *AtAUX1* and has proven to be particularly important for protein function (Swarup et al. 2004). In addition, both *curl-1* and *curl-3* mutations (Fig. 5D) are located in TM helix IV (Supplementary Fig. S5B), which is in the similar part of the N-terminal half of AtAUX1 and is essential for its correct localization (Peret et al. 2012). The *curl-7* mutant has only five TM helixes, losing the rest five TM helixes (Supplementary Fig. S5D). Furthermore, the *curl-1/curl-3*, *curl-2/curl-6*, and *curl-7* mutations caused nonsense mutations that can produce only 35, 63, and 45% of the WT protein, respectively (Fig. 5B, D, and 6D). Additionally, the relative expression of the *curl* mutant alleles (*curl-1*, *curl-2,* and *curl-6*) was less than 40% compared to that of WT (Fig. 5F). These reasons presumably account for the loss-of-function mutations of the *SlLAX1* gene.

To test the potential function of SlLAX1 as an auxin transporter, we first measured leaf endogenous auxin content. However, IAA content was comparable between WT and the *curl* mutants at all stages (Supplementary

Fig. S3). Numerous findings have indicated that *AtAUX1* plays an important role in root gravitropism and lateral root development (Bennet et al. 1996, Marchant et al. 1999). Root gravitropism response is also commonly used to check auxin response and distribution. Therefore, we next tested these assays and found that the root gravitropism response of the *curl* mutants was affected by the *SlLAX1* mutation. In addition, lateral root emergence was also disrupted (Supplementary Fig. S4). Although the functional characterization of SlLAX1 has not been conducted in tomato and we do not yet have direct evidence in this study, agravitropism and lateral root formation defects of the *curl* mutants indicated that SlLAX1 may have a potential function as an auxin transporter similar to AtAUX1, and SlLAX1 might participate in local auxin distribution without affecting total endogenous auxin content of the whole leaf. Functional analysis of *SlLAX1* gene remains to be determined.

Curly leaf phenotype of the *curl* mutants is presumably caused by an imbalance of pavement cell enlargement between adaxial and abaxial side

The curly leaf phenotype was not observed at the early stage of leaf development (Fig. 1C, D, Supplementary Fig. S1), and does not related to relative humidity and water availability (Fig. 1 E, G). Thus, we hypothesized that the curly leaf phenotype was caused by the alteration of adaxial/abaxial cell ratio rather than impairment adaxial-abaxial polarity since adaxial-abaxial polarity is established at the very early stage of leaf development, that is, at the primordium stage. As expected, pavement cell size in the abaxial in the *curl* mutants was significantly larger compared to that of WT, while there was no significant difference in the adaxial side. The number of pavement cell in adaxial and abaxial sides was comparable. The upward curling of the *curl* mutants might be explained by the differential growth of pavement cells in adaxial and abaxial cell surfaces, which is supported by similar observation of *incurvata6* (*icu6*), semi-dominant allele of the *AUXIN RESISTANT3* (*AXR3*), that showed an upward curly phenotype caused by a reduced adaxial/abaxial cell size ratio (Perez-Perez et al. 2010). The imbalance epidermal adaxial-abaxial cell growth which led to either epinastic (downward curvature) or hyponastic leaf is not new phenomenon. In previous finding, it was reported that auxin hyper accumulation plant produced leaf epinastic curvature that was formed due to an increased growth of the leaf adaxial side (Klee et al. 1987, Romano et al. 1993, Kim et al. 2007), that induced by reduced auxin export that may cause its hyper-accumulation on the adaxial side. Taken together, SlLAX1 might have a function not in the establishment of adaxial-abaxial polarity but rather in balancing adaxial/abaxial cell size ratio in later stages of leaf development. The evaluation of auxin distribution and/or analysis of *SlLAX1* gene expression on adaxial and abaxial leaf surfaces should allow for a better understanding of the *SlLAX1* function in this process.

According to the relative expression of some tomato putative auxin-related genes controlling leaf flatness, *SlYuc1* showed prominent changes in both young and mature leaves of the *curl* mutants. *YUC* is a family of genes that are orthologs to *ToFZY* (Expo´sito-Rodrı´guez et al. 2007), which has a function in local auxin biosynthesis (Zhao et al. 2001). In the previous finding, it has been reported that *aux1* and *yuc* mutants in *Arabidopsis* have a synergistic effect to enhance each other to control leaf development. Lower expression of *SlYuc1* does not change leaf auxin content presumably because *SlYuc* is family genes (Expósito-Rodríguez et al. 2007). Other *SlYuc* genes may compensate total auxin biosynthesis, resulting in comparable amounts of auxin content in entire leaf. In *Arabidopsis*, activation tagging of *AtDof5.1* resulted in an upward curly leaf phenotype (Kim et al. 2010). Dof5.1 was demonstrated to promote the *Revoluta* gene expression by binding to its promoter. Similar to these finding (Kim at al. 2010), expression of *SlDof25,* an ortholog of *Dof5.1,* was increased in the all *curl* mutants (Fig. 8G). The *SlRev* expression level was also increased (Fig. 8L). Up regulation of *AtDof5.1* also repressed transcript levels of auxin biosynthesis genes, which is consistent with low expression level of *SlYuc1* in the *curl* mutants (Fig. 8D, J). In tomato, it has also been reported that overexpression of a microRNA166-resistant version of *SLREV* (35S::REV^{Ris}) showed upward curly leaf phenotype (Hu et al. 2014). Collectively, our findings are similar to previous findings which reinforce the partial disturbance of auxin homeostasis in the *SlLAX1* mutants.

The fact that lower auxin content triggers cell expansion is well established (Ishida et al. 2012, reviewed in Velasquez et al. 2016). We hypothesize that the loss-of-function of *SlLAX1* in the *curl* mutants results in imbalanced adaxial/abaxial pavement cell growth leading to curly leaf phenotype. Depletion of SlLAX1 in the *curl* mutants disrupts auxin transport in either adaxial or abaxial leaf surface. Given that there was no significant difference in the adaxial pavement cell size (Table 6, Fig 7A), SlLAX1 action appears to be restricted to the abaxial side. SlLAX1 belongs to the SlLAXs family and other members are known to be expressed in leaves (Pattison and Catala, 2012). It is possible that other influx transporters compensate for the loss-of-function of SlLAX1 in the adaxial side. In contrast, our data suggest that SlLAX1 is a major determinant of auxin transportation dominant in the abaxial side. In adaxial side, where SlLAX1 is not a major auxin influx carrier, presumably auxin content of the *curl* mutants was similar or higher than that of the WT, while decreased auxin content in abaxial side due to low influx carrier activity. Auxin which is not uptake by abaxial cell, may be accumulated in the adaxial side, or alternatively accumulated in the extracellular space (most likely the latter because the cell number in the adaxial and abaxial was comparable, means there was no increase of cell division in adaxial). Therefore, the auxin content in the *curl* mutants could be maintained at the similar level with the WT

(Supplementary Fig. S3). Imbalanced adaxial/abaxial cell growth due to differential auxin accumulation is also well established (Perez-Perez et al. 2010, reviewed in Sandalio et al. 2016). We speculate that the lower auxin content in abaxial cell surface triggers cell expansion and imbalanced cell growth in both surface leading to curly leaf emergence. This hypothesis awaits further investigation.

In brief, this study contributes to the newly characterized role of *SlLAX1* in controlling leaf development in tomato by balancing the adaxial-abaxial pavement cell enlargement potentially mediated by auxin. The evaluation of auxin distribution and/or analysis of *SlLAX1* gene expression on adaxial and abaxial leaf surfaces should allow for a better understanding of the *SlLAX1* function in this process. Additionally, analysis of double mutants with other *LAX* or *PIN* family members and other adaxial-abaxial-specification genes would be helpful to dissect the precise mechanism of *SlLAX1* in normal leaf development in plants.

Materials and methods

Plant material and growth conditions

Tomato (*Solanum lycopersicum* cv. 'Micro-Tom') curly leaf (*curl*) mutants were generated by EMS and γ-ray irradiation. The mutants were obtained from the National BioResources (NBRP) Project at the University of Tsukuba (Saito et al. 2011, Shikata et al. 2016). From the M_3 mutagenized population, we isolated six lines of the curly leaf phenotype mutants, herein referred to as '*curl*' mutants. The mutant screening was carried out visually using mature plants showing severe curly leaf phenotypes. Five mutant alleles, *curl 1-5*, were generated by γ-ray irradiation, and one mutant allele, *curl-6*, was generated by EMS mutagenesis. Furthermore, using TILLING screening, we screened another EMS mutant, *curl-7*. These mutants were registered in the TOMATOMA mutant database (Saito et al. 2011, http://tomatoma.nbrp.jp/). The NBRP accession numbers are listed in Supplementary Table S6. Unless otherwise stated, further analyses of the *curl* mutants were conducted after two backcrosses to the WT 'Micro-Tom' to remove any possible background mutation following the mutagenesis treatment. The plants were grown under standard cultivation conditions in the greenhouse facility at the University of Tsukuba.

Genomic DNA extraction, construction of mapping population, DNA marker, and genetic analysis

Genomic DNA was extracted from 2-month-old plants. A maximum of 100 mg of fresh leaf sample was extracted using a Maxwell® 16 Tissue DNA Purification Kit (Promega, Madison, USA). To perform rough mapping using DNA markers, *curl-2* was crossed to another tomato cultivar, 'Ailsa Craig,' to obtain a mapping population. From approximately 100 plants of the F_2 mapping population, 19 plants exhibiting the curly mutant phenotype were

isolated, and genomic DNA was extracted from the leaves of the individual plants. These plants were subjected to rough mapping experiments. All SNP and CAPS DNA markers were designed according to the AMF_2 (F_2: *S. lycopersicum* 'Ailsa Craig' x *S. lycopersicum* 'Micro-Tom') linkage map information that publicly available from the Kazusa DNA Research Institute (KDRI) webpage (http://marker.kazusa.or.jp/Tomato/, Shirasawa et al. 2010). The primers and restriction enzyme used in the rough mapping chromosome are listed in Supplementary Table S7.

Exome sequence and variant identification

ES was performed to narrow down the candidate genes. Four alleles, *curl-1*, *curl-2*, *curl-3*, and *curl*-6, of the *curl* mutants of the F_2 mutant population backcrossed to the WT were used. The mutants and WT phenotypes were selected in the F_2 population based on the presence or absence of curly leaves among approximately 100 F_2 plants for each line, after which their DNA samples were bulked based on phenotype. Exome sequence analysis was then performed based on the Roche exome sequence SeqCap® EZ SR protocol (http://sequencing.roche.com/).

Briefly, genomic DNA was treated with a Covaris® S220 Ultrasonicator (Covaris, Massachusetts, USA) to achieve an average length of 200 bp. Then, a multiplex NGS library was constructed using a KAPA® Library Preparation Kit and SeqCap® adapter kit (Roche, Basel, Switzerland). After constructing the NGS library, exome capture was conducted using a custom probe set that was designed based on the tomato genome reference version SL2.40 (supporting dataset, Sol Genomics Network, https://solgenomics.net). This probe set was designed to capture 49.5 Mb of exonic DNA regions (Supplementary Data S1). The resultant exome library was amplified by 14 cycles of post-capture ligation-mediated PCR with KAPA HiFi HostStart ReadyMix (Roche) and then subjected to Illumina HiSeq-2000 sequencing set to the 100-bp paired-end mode. Paired-end short read data were subjected to quality filtering using FASTXToolkit with the parameters of –Q 20 –P 90. Then, short reads were aligned to the tomato genome reference version SL2.50 using bowtie2 software with the following parameters: L,0,-0.16 --mp 2,2 --np 1 --rdg 1,1 --rfg 1,1. On average, 98.8 ± 0.03% of the target exonic regions were covered by short reads. The average read depth was 18 ± 1.5. Genome-wide DNA polymorphisms and mutations were identified based on the alignment results by the HaplotypeCaller function of the Genome Analysis Toolkit (GATK) with the following parameters: -mmq 5 -forceActive -stand_call_conf 10 -stand_emit_conf 10. The resultant DNA variant information was further combined into one genomic VCF dataset with the GenotypeGVCFs function of the GATK. Three wild-type ES datasets (accession No. DRR097500 to DRR097502, DNA Data Bank of Japan (DDBJ)), two wild-type whole-genome NGS datasets (DDBJ accession

No. DRR097503 and DRR097504), and one publicly available wild-type whole-genome NGS dataset (Kobayashi et al. 2014) were used as controls to remove intra-cultivar variations that are present between WT 'Micro-Tom' lines. DNA variants were further removed if their allele frequencies exceeded >90% in the WT F_2 bulked segregants because they were also expected to be intra-cultivar variations. Those variants with < 20% allele frequency or with a read depth < 6 were also removed because they were likely to be false-positives. ES datasets for *curl* mutants are available in DDBJ (accession No. DRR097492 to DRR097502).

RNA extraction and cDNA synthesis

Total RNA was extracted from young and mature leaves (when the leaves were completely curly) using an RNeasy Mini Kit (QIAGEN) according to the manufacturer's protocol. To remove genomic DNA contamination, two steps were applied: an on-column RNase-free DNase Set (QIAGEN) and an RNA Clean & Concentrator™-5 (Zymo Research). Subsequently, cDNA was synthesized from 2000 ng of total RNA by a SuperScript III First Strand Synthesis Kit (Invitrogen, Thermo Fisher Scientific, USA) according to the manufacturer's instructions.

Cloning and sequencing of the full-length coding sequence the *SlAX1* gene

The full-length coding sequence (1236 bp) of the *SlAX1* gene from three independent plants was amplified by PCR. The primer sequences are listed in Supplementary Table S4. Subsequently, PCR products were loaded onto a 0.8–1.5% agarose gel, which was then electrophoresed for 45-60 min. Next, the band was visualized under 70% UV and then cut either with a gel cutter or blade. Any visible desired product band was individually cut, removed, and subsequently subjected to purification using a Wizard® SV Gel and PCR Clean-Up System (Promega, Madison, USA). DNA purification by centrifugation was applied. The purified PCR product was then cloned into the entry vector pCR8/GW/TOPO (Invitrogen, http://www.lifetechnologies.com/) using an In-Fusion® HD Cloning Kit (Takara Bio USA, Inc.) according to the manufacturer's protocol. Then, plasmids from clones were purified using a FastGene Plasmid Mini Kit (Nippon Genetics, Japan). The plasmid fragments were sequenced using M13 primers (Supplementary Table S4).

qRT-PCR analysis

mRNA expression level was quantified using qRT-PCR. A 10 ng/µl cDNA template of three biological replicates was used for gene expression analyses. The *SlActin* gene was used as an internal control (Lovdal and Lillo. 2009). qRT-PCR was carried out using a CFX96 Real-Time System (Bio-Rad) with SYBR Premix ExTaq

II (Ili RNase H Plus; TaKaRa Bio, Japan). The primers used for qRT-PCR are listed in the Supplementary Table S4. Relative gene expression was quantified using the $\Delta\Delta C_T$ method (Pfaffl 2001). The qRT-PCR mixture reaction and thermal cycle conditions were as described by Shinozaki et al. (2015). The primers for qRT-PCR were designed using the Primer3 Plus website (http://primer3plus.com/); two exons in the forward and primer were joined to exclude any possibility of contamination of genomic DNA.

Screening new *SlLAX1* mutant alleles by TILLING

The TILLING population was previously described by Okabe et al. (2013), and the TILLING experiments were performed as described by Okabe et al. (2011). We attempted to screen for mutations in the coding region of the *SlLAX1* gene. The primer pair was designed to span exon 6. Given that exon 6 is the longest exon, we also identified an EMS mutant line, *curl-6*, that carries a nonsense mutation in exon 6 of *SlLAX1*. The primer pairs used in the TILLING experiment were forward 5'-TGGTACATGGGAACTAGCTAAGCC-3' and reverse 5'-ACCTGACGAGCGGATGATTTTC-3,' which amplified 865 bp of genomic DNA template; the 5' end of each primer was labeled with DY-681 or DY-781, which are equivalent to IRDye 700 or IRDye 800 (https://www.biomers.net/), respectively.

Morphological analysis

The curvature index (CI) of mutants was measured in accordance with the method introduced by Liu et al. (2010) on the 5th leaflet. Leaf area and perimeter analyses were conducted at the young and mature leaf stages; 15 leaves harvested from the same position were used as samples. Leaf images were captured using a digital camera, and the leaf area and perimeter were measured using CellSensStandard imaging software (Olympus, Japan). The leaf perimeter and leaf area were measured by following the edge of the leaf using a closed polygon measurement tool within the CellSensStandard software. The reduction in leaf area and leaf perimeter (%) were measured by comparing the values before flattening and the values after flattening (multiplied by 100).

Scanning electron microscope (SEM) experiment

The leaf epidermal surface was observed using a scanning electron microscope (Hitachi Tabletop Microscope TM3000, Japan). The cell feature was measured at the mature leaf stage when the leaves were completely turned to curly, precisely in the same regions on adaxial and abaxial surfaces. Mature fresh leaves were sampled and flattened before being subjected to microscopic observation. Approximately 0.5 x 0.5 cm^2 of adaxial or abaxial

surface was placed into a sample box, after which the epidermal pavement cell was imaged at 400x magnification for at least three biological replications. The cell size was quantified separately using CellSensStandard software. All measurements were obtained for at least three independently captured SEM images for each replication and three fields of view for each image.

For the number of pavement cell quantification, leaf samples were cut from midway precisely between the midrib to the margin of fully curly leaves. We used precisely the same position both in adaxial and in abaxial side, one side was used for adaxial pavement cell observation, and the other was used for abaxial. About 2-4 mm leaf sample in the tip area of transversal axis was cut irrespective the size from the midrib to the margin, and it was subjected to SEM experiment (Supplementary Fig. S6). The cell number was counted thoroughly in that region. Measurements were obtained from three biological replications.

Measurement of the auxin content in leaves

Leaves were sampled at three stages from the same positions at (i) young leaves, before curly leaves formed (ii) when leaves just turned into curly; and (iii) mature leaves, after leaves were fully curly. Three biological replications were included at each stage. At least 100 mg of fresh leaves was immediately frozen in liquid nitrogen and crushed into a fine powder using a TissueLyser (Qiagen, Germany). Endogenous auxin was measured using a UHPLC-Q-Exactive (Thermo Fisher Scientific) system. Measurements were conducted as described by Kojima et al. (2009) and Shinozaki et al. (2015).

Leaf water potential measurements

Leaf water potential was measured using a pressure chamber. A leaflet from the same position was cut and immediately placed into the chamber. Pressure was gradually increased until water was exuded from the petiole. Six biological samples were tested.

Statistical analysis

Unless otherwise stated, the data are presented as the mean ± SE (standard error). Student's *t*-test (at the 95 and 99% significance levels) was used to analyze the significance level between two values with equal variance. Chi-square (χ^2) tests were performed using MS Excel 2016 to examine the goodness of fit between the expected and observed Mendelian ratio in the segregating F_2 population of mutants backcrossed to the WT 'Micro-Tom,' and the degrees of freedom and expected Mendelian ratio used for monogenic traits were 1 and 3:1 (WT: mutant

phenotype), respectively.

Funding

This work was supported by JSPS KAKENHI Grant-in-Aid for Research Activity start-up [15H06071 to RY], Program to Disseminate Tenure Tracking System to TA, and the Japan Advanced Plant Science Network to HE and HS.

Disclosures

The authors declare that they have no conflict of interest.

Acknowledgements

Tomato 'Micro-Tom' and the *curl* mutant seeds were obtained from the National BioResource Project (NBRP), Ministry of Education, Culture, Sports, Science and Technology (MEXT), Japan. We are grateful for helpful comments and discussion on the manuscript from Dr. Kentaro Ezura. We would like to express our sincere gratitude to all our laboratory members for their great support and helpful discussion throughout the work.

References

Ariizumi, T., Kishimoto, S., Kakami, R., Maoka, T., Hirakawa, H., Suzuki, Y., et al. (2014) Identification of the carotenoid modifying gene *PALE YELLOW PETAL 1* as an essential factor in xanthophyll esterification and yellow flower pigmentation in tomato (*Solanum lycopersicum*). *Plant J*. 79: 453–465.

Bainbridge, K., Guyomarc'h, S., Bayer, E., Swarup, R., Bennett, M., Mandel, T., et al. (2008) Auxin influx carriers stabilize phyllotactic patterning. *Genes Dev*. 22: 810–823.

Bennett, M.J., Marchant, A., Green, H.G., May, S.T., Ward, S.P., Millner, P.A., et al. (1996) *Arabidopsis AUX1* Gene: A permease-like regulator of root gravitropism. *Science* 273: 948–950.

Bennett, M.J., Marchant, A., May, S.T., and Swarup, R. (1998) Going the distance with auxin: unravelling the molecular basis of auxin transport. *Philos. Trans. R. Soc. Lond. B. Biol. Sci*. 353: 1511–1515.

Cai, X., Zhang, Y., Zhang, C., Zhang, T., Hu, T., Ye, J., et al. (2013) Genome-wide Analysis of plant-specific Dof transcription factor family in tomato. *J. Integr. Plant Biol*. 55: 552–566.

Cheng, Y., Dai, X., and Zhao, Y. (2007) Auxin synthesized by the YUCCA flavin monooxygenases is essential for embryogenesis and leaf formation in *Arabidopsis*. *Plant Cell* 19: 2430–2439.

Chusreeaeom, K., Ariizumi, T., Asamizu, E., Okabe, Y., Shirasawa, K., and Ezura, H. (2014) A novel tomato mutant, *Solanum lycopersicum elongated fruit1* (*Slelf1*), exhibits an elongated fruit shape caused by increased cell layers in the proximal region of the ovary. *Mol. Genet. Genomics* 289: 399–409.

Delbarre, A., Muller, P., Imhoff, V., and Guern, J. (1996) Comparison of mechanisms controlling uptake and accumulation of 2,4-dichlorophenoxy acetic acid, naphthalene-1-acetic acid, and indole-3-acetic acid in suspension-cultured tobacco cells. *Planta* 198: 532–541.

Emery, J.F., Floyd, S.K., Alvarez, J., Eshed, Y., Hawker, N.P., Izhaki, A., et al. (2003) Radial patterning of *Arabidopsis* shoots by class III HD-ZIP and KANADI genes. *Curr. Biol.* 13: 1768–1774.

Esteve-Bruna, D., Perez-Perez, J.M., Ponce, M.R., and Micol, J.L. (2013) *incurvata13*, a novel allele of *AUXIN RESISTANT6*, reveals a specific role for auxin and the SCF complex in *Arabidopsis* embryogenesis, vascular specification, and leaf flatness. *Plant Physiol*. 161: 1303–1320.

Expósito-Rodríguez, M., Borges, A.A., Borges-Pérez, A., Hernández, M., and Pérez, J.A. (2007) Cloning and biochemical characterization of *ToFZY*, a tomato gene encoding a flavin monooxygenase involved in a tryptophan-dependent auxin biosynthesis pathway. *J. Plant Growth Regul*. 26: 329–340.

Fàbregas, N., Formosa-Jordan, P., Confraria, A., Siligato, R., Alonso, J.M., Swarup, R., et al. (2015) Auxin influx carriers control vascular patterning and xylem differentiation in *Arabidopsis thaliana*. *PLoS Genet*. 11: 1–26.

Hao, S., Ariizumi, T., and Ezura, H. (2017) *SEXUAL STERILITY* is essential for both male and female gametogenesis in tomato. *Plant Cell Physiol*. 58: 22–34.

Hu, G., Fan, J., Xian, Z., Huang, W., Lin, D., and Li, Z. (2014) Overexpression of *SlREV* alters the development of the flower pedicel abscission zone and fruit formation in tomato. *Plant Sci.* 229: 86-95.

Ishida, T., Adachi, S., Yoshimura, M., Shimizu, K., Umeda, M., and Sugimoto, K. (2010) Auxin modulates the transition from the mitotic cycle to the endocycle in *Arabidopsis*. *Development*. 137: 63–71.

Kasprzewska, A., Carter, R., Swarup, R., Bennett, M., Monk, N., Hobbs, J.K., et al. (2015) Auxin influx importers modulate serration along the leaf margin. *Plant J*. 83: 705–718.

Kim, H.S., Kim, S.J., Abbasi, N., Bressan, R.A., Yun, D.J., Yoo, S.D., et al. (2010) The DOF transcription factor Dof5.1 influences leaf axial patterning by promoting *Revoluta* transcription in *Arabidopsis*. *Plant J*. 64: 524–535.

Kim, J.I., Sharkhuu, A., Jin, J.B., Li, P., Jeong, J.C., Baek, D., et al. (2007) *yucca6*, a dominant mutation in *Arabidopsis*, affects auxin accumulation and auxin-related phenotypes. *Plant Physiol*. 145: 722–735.

Klee, H.J., Horsch, R.B., Hinchee, M.A., Hein, M.B., and Hoffmann, N.L. (1987) The effects of overproduction of two *Agrobacterium tumefaciens* T-DNA auxin biosynthetic gene products in transgenic petunia plants. *Genes Develop*. 1: 86–96.

Kobayashi, M., Nagasaki, H., Garcia, V., Just, D., Bres, C., Mauxion, L.P., et al. (2014) Genome-wide analysis of intraspecific DNA polymorphism in 'Micro-Tom', a model cultivar of tomato (*Solanum lycopersicum*). *Plant Cell Physiol*. 55: 445–454.

Kojima, M., Kamada-Nobusada, T., Komatsu, H., Takei, K., Kuroha, T., Mizutani, M., et al. (2009) Highly sensitive and high-throughput analysis of plant hormones using MS-probe modification and liquid chromatography – tandem mass spectrometry: an application for hormone profiling in *Oryza sativa*. *Plant Cell Physiol*. 50: 1201–1214.

Kramer, E.M., and Bennett, M.J. (2006) Auxin transport: a field in flux. *Trends Plant Sci*. 11: 382–386.

Lee, C., Chronis, D., Kenning, C., Peret, B., Hewezi, T., Davis, E.L., et al. (2011) The novel cyst nematode effector protein 19C07 interacts with the *Arabidopsis* auxin influx transporter LAX3 to control feeding site development. *Plant Physiol*. 155: 866–880.

Liu, Z., Jia, L., Mao, Y., and He, Y. (2010) Classification and quantification of leaf curvature. *J. Exp. Bot*. 61: 2757–2767.

Liu, Z., Jia, L., Wang, H., and He, Y. (2011) HYL1 regulates the balance between adaxial and abaxial identity for leaf flattening via miRNA-mediated pathways. *J. Exp. Bot*. 62: 4367–4381.

Løvdal, T., and Lillo, C. (2009) Reference gene selection for quantitative real-time PCR normalization in tomato subjected to nitrogen, cold, and light stress. *Anal. Biochem*. 387: 238–242.

Marchant, A., Bhalerao, B., Casimiro, I., Eklöf, J., Casero, P.J., Bennett, M., et al. (2002) AUX1 promotes lateral root formation by facilitating indole-3-acetic acid distribution between sink and source tissues in the *Arabidopsis* seedling. *Plant Cell* 14: 589–597.

Marchant, A., Kargul, J., May, S.T., Muller, P., Delbarre, A., Perrot-Rechenmann, C., et al. (1999) AUX1 regulates root gravitropism in *Arabidopsis* by facilitating auxin uptake within root apical tissues. *EMBO J*. 18: 2066–2073.

Newman, K.L., Fernandez, A.G., and Barton, M.K. (2002) Regulation of axis determinacy by the *Arabidopsis PINHEAD* gene. *Plant Cell* 14: 3029–3042.

Okabe, Y., Ariizumi, T., and Ezura, H. (2013) Updating the Micro-Tom TILLING platform. *Breed. Sci*. 63: 42–48.

Okabe, Y., Asamizu, E., Saito, T., Matsukura, C., Ariizumi, T., Bres, C., et al. (2011) Tomato TILLING technology: Development of a reverse genetics tool for the efficient isolation of mutants from Micro-Tom mutant libraries. *Plant Cell Physiol*. 52: 1994–2005.

Paciorek, T., Zažímalová, E., Ruthardt, N., Petrášek, J., Stierhof, Y.-D., Kleine-Vehn, J., et al. (2005) Auxin inhibits endocytosis and promotes its own efflux from cells. *Nature* 435: 1251–1256.

Pattison, R.J., and Catalá, C. (2012) Evaluating auxin distribution in tomato (*Solanum lycopersicum*) through an analysis of the *PIN* and *AUX/LAX* gene families. *Plant J*. 70: 585–598.

Peret, B., Rybel, B.D, Casimiro, I., Benkova, E., Swarup, R., Laplaze, L., et al. (2009) Arabidopsis lateral root development: an emerging story. *Trends Plant Sci*. 14: 399–408.

Peret, B., Swarup, K., Ferguson, A., Seth, M., Yang, Y., Dhondt, S., et al. (2012) *AUX/LAX* genes encode a family of auxin influx transporters that perform distinct functions during *Arabidopsis* development. *Plant Cell* 24: 2874–2885.

Pérez-Pérez, J.M., Candela, H., Robles, P., López-Torrejón, G., Del Pozo, J.C., and Micol, J.L. (2010) A role for AUXIN RESISTANT3 in the coordination of leaf growth. *Plant Cell Physiol*. 51: 1661–1673.

Pfaffl, M.W. (2001) A new mathematical model for relative quantification in real-time RT-PCR. *Nucleic Acids Res*. 29: e4516–e4521.

Prigge, M.J., Otsuga, D., Alonso, J.M., Ecker, J.R., Drews, G.N., and Clark, S.E. (2005) Class III homeodomain-leucine zipper gene family members have overlapping, antagonistic, and distinct roles in *Arabidopsis* development. *Plant Cell* 17: 61–76.

Romano, C.P., Cooper, M.L., and Klee, H.J. (1993) Uncoupling auxin and ethylene effects in transgenic tobacco and *Arabidopsis* plants. *Plant Cell* 5: 181–189.

Rutschow, H.L., Baskin, T.I., and Kramer, E.M. (2014) The carrier AUXIN RESISTANT (AUX1) dominates auxin flux into *Arabidopsis* protoplasts. *New Phytol*. 204: 536–544.

Sagar, M., Chervin, C., Mila, I., Hao, Y., Roustan, J.-P., Benichou, M., et al. (2013) SlARF4, an auxin response factor involved in the control of sugar metabolism during tomato fruit development. *Plant Physiol*. 161: 1362–1374.

Saito, T., Ariizumi, T., Okabe, Y., Asamizu, E., Hiwasa-Tanase, K., Fukuda, N., et al. (2011) TOMATOMA: A novel tomato mutant database distributing Micro-Tom mutant collections. *Plant Cell Physiol*. 52: 283–296.

Sandalio, L.M., Godiguez-Serrano, M, and Romero-Puertas, M.C. (2016) Leaf epinasty and auxin: A biochemical and molecular overview. *Plant Sci*. 253: 187-193.

Serrano-Cartagena, J., Robles, P., Ponce, M.R., and Micol, J.L., (1999). Genetic analysis of leaf form mutants from the *Arabidopsis* information service collection. *Mol. Gen. Genet.* 261: 725–739.

Shikata, M., Hoshikawa, K., Ariizumi, T., Fukuda, N., Yamazaki, Y., and Ezura, H. (2016) TOMATOMA update: Phenotypic and metabolite information in the Micro-Tom mutant resource. *Plant Cell Physiol*. 57: e11 1-10.

Shinozaki, Y., Hao, S., Kojima, M., Sakakibara, H., Ozeki-Iida, Y., Zheng, Y., et al. (2015) Ethylene suppresses tomato (*Solanum lycopersicum*) fruit set through modification of gibberellin metabolism. *Plant J*. 83: 237–251.

Shirasawa, K., Isobe, S., Hirakawa, H., Asamizu, E., Fukuoka, H., Just, D., et al. (2010) SNP discovery and linkage map construction in cultivated tomato. *DNA Res*. 17: 381–391.

Song, J.B., Huang, S.Q., Dalmay, T., and Yang, Z.M. (2012) Regulation of leaf morphology by microRNA394 and its target *LEAF CURLING RESPONSIVENESS*. *Plant Cell Physiol*. 53: 1283–1294.

Swarup, K., Benková, E., Swarup, R., Casimiro, I., Péret, B., Yang, Y., et al. (2008) The auxin influx carrier LAX3 promotes lateral root emergence. *Nat. Cell Biol*. 10: 946-954.

Swarup, R. (2004) Structure-function analysis of the presumptive Arabidopsis auxin permease AUX1. *Plant Cell* 16: 3069–3083.

Swarup, R., and Péret, B. (2012) AUX/LAX family of auxin influx carriers-an overview. *Front. Plant Sci*. 3: 1–11.

Tromas, A., and Perrot-Rechenmann, C. (2010) Recent progress in auxin biology. *Comptes Rendus - Biol*. 333: 297–306.

Velasquez, S.M., Elke, B., Jürgen K., and José M. E. (2016) Auxin and cellular elongation. *Plant Physiol.* 70: 1206-1215.

Vieten, A., Sauer, M., Brewer, P.B., and Friml, J. (2007) Molecular and cellular aspects of auxin-transport-mediated development. *Trends Plant Sci*. 12: 160–168.

Yang, H., and Murphy, A.S. (2009). Functional expression and characterization of *Arabidopsis* ABCB, AUX 1 and PIN auxin transporters in *Schizosaccharomyces pombe*. *Plant J*. 59: 179–191.

Yu, L., Yu, X., Shen, R., and He, Æ.Y. (2005) *HYL1* gene maintains venation and polarity of leaves. *Planta* 221: 231–242.

Zgurski, J.M., Sharma, R., Bolokoski, D.A., and Schultz, E.A. (2005) Asymmetric auxin response precedes asymmetric growth and differentiation of *asymmetric leaf1* and *asymmetric leaf2 Arabidopsis* leaves. *Plant Cell* 17: 77–91.

Zhao, Y., Christensen, S. K., Fankhauser, C., Cashman, J.R., Cohen, J. D., Weigel. D., et al. (2001) A role for flavin monooxygenase-like enzymes in auxin biosynthesis. *Science* 291: 306–309.

Table 1 Leaf area and leaf perimeter of young and mature leaves of the *curl* mutants.

Line	Young leaf						Mature leaf					
	Leaf area			Leaf perimeter			Leaf area			Leaf perimeter		
	Before flattening (mm^2)	After flattening (mm^2)	Reduction (%)	Before flattening (mm)	After flattening (mm)	Reduction (%)	Before flattening (mm^2)	After flattening (mm^2)	Reduction (%)	Before flattening (mm)	After flattening (mm)	Reduction (%)
WT	685.2±47.7	662.0±40.4	3.5	125.7±5.6	124.6±5.7	0.9	1489.2±63.2	1440.4±57.3	3.4	188.1±4.3	190.0±5.8	-1.0
curl-1	397.1±54.7**	694.3±45.4	-42.8	119.3±3.7	118.9±3.9	0.3	530.4±72.9**	1471.8±77.1	-64.0	175.0±7.9	191.3±7.8	-8.6
curl-2	289.3±54.3**	664.9±24.1	-56.5	130.1±3.1	129.4±2.4	0.5	314.9±70.4**	1362.1±98.0	-76.9	180.6±5.9	190.7±7.2	-5.3
curl-6	316.6±27.7**	649.7±36.1	-51.3	121.1±5.3	118.4±3.5	2.3	697.2±81.6**	1575.5±122.7	-55.8	189.9±9.2	214.7±11.3	-11.6

Young leaf area and perimeter were observed when the curly leaf was being progressed, about six days after leaf initiation. Mature leaf's leaf area and perimeter were observed when leaf completely become curly, about ten days after leaf initiation.

Values are means ± SE (n=15). The asterisks represent statistically significant differences in means with equal variants based on Student's t-test ($^{**}P<0.01$), wild-type mean values was used as controls. The reduction in leaf area and leaf perimeter (%) were measured by comparing the values before flattening and the values after flattening (multiplied by 100).

Table 2 The global curvature of the young and mature leaves of the *curl* mutants.

Young leaf						Mature leaf					
Line	Direction	Axis	Transverse CI	Longitudinal CI	Extent	Line	Direction	Axis	Transverse CI	Longitudinal CI	Extent
WT	flat	-	0.0 ± 0.0	0.0 ± 0.0	-	WT	flat	-	0.0 ± 0.0	0.00 ± 0.0	-
curl-1	upward	transverse	-0.3 ± 0.0**	0.0 ± 0.0	low	*curl-1*	upward	transverse	-0.7 ± 0.2**	-0.02 ± 0.0	high
curl-2	upward	transverse	-0.2 ± 0.0**	0.0 ± 0.0	1ow	*curl-2*	upward	transverse	-0.8 ± 0.2**	0.00 ± 0.0	high
curl-6	upward	transverse	-0.3 ± 0.0**	0.0 ± 0.0	low	*curl-6*	upward	transverse	-0.8 ± 0.2**	-0.01 ± 0.0	high

Values are means ± SE (*n*=15). Curvature index (CI) of mutants was measured by a method introduced by Liu et al. 2010.
CI= (ab-a'b')/ab
CI= curvature index
ab= the distance between points *a* and *b* on two margins of curvature before flattening of leaves
a'b' = the distance between *a* and *b* on two margins after flattening
Negative (-) CI represents upward curvature.
Values are means ± SE (*n*=15). The asterisks represent statistically significant differences in means with equal variants based on Student's *t*-test (**P<0.01).
The curvature index was measured in the middle of the leaves. The flatness of either young or mature leaf *curl* mutants was impaired along the transverse axis, whereas the longitudinal axis was normal.

Table 3 Segregation analysis of the *curl* mutants back-crossed to the wild-type 'Micro-Tom'.

Mutant line[a]	F_1[b] WT: curly	F_2[b] WT: curly	χ^2 value[c]	χ^2 reference[d]	*P*-value	Inheritance pattern[e]
curl-1	4:0	105:25	2.30	3.84	0.13	monogenic recessive
curl-2	1:0	79:31	0.59	3.84	0.44	monogenic recessive
curl-3	5:0	70:25	0.08	3.84	0.76	monogenic recessive
curl-6	2:0	123:30	2.37	3.84	0.12	monogenic recessive

[a] The *curl* mutants were crossed to the wild-type 'Micro-Tom'.
[b] The number of progeny exhibiting normal (WT) and curly leaf phenotype is shown.
[c] χ^2 value was calculated based on progeny segregation in the F_2 population.
[d] χ^2 distribution in the table reference value, with probability >0.05, and degree of freedom 1.
[e] Inheritance pattern of the curl mutants, estimated based on χ^2 value at 95% ($P<0.05$) significant level.

Table 4 The result of the allelism test among the *curl* mutants.

Mutant line ♀	Mutant line ♂					
	WT	*curl-1*	*curl-2*	*curl-3*	*curl-4*	*curl-6*
WT		normal	normal	normal	normal	normal
curl-1	normal		n.d.	n.d.	n.d.	curly
curl-2	normal	curly		n.d.	n.d.	curly
curl-3	normal	n.d.	curly		curly	curly
curl-4	normal	n.d.	curly	curly		curly
curl-6	normal	curly	curly	curly	curly	

The allelism test was carried out by crossing all possible pairs and observing the results at the F_1 generation.
The F_1 generation phenotype was evaluated visually by observing the presence of a curly leaf phenotype.
Normal represents the wild-type phenotype
Curly represents the curly leaf phenotype.
n.d. not determined.
♀, ♂: female recipient and male donor, respectively.

Table 5 Predicted mutation position, amino acid substitution, and mutation type based on the whole exome sequence result.

Chromosome[a]	Position[b] (bp)	REF nuc[c]	ALT nuc[d]	Within[e]	Gene[f]	Strand	Amino acid substitution	Mutation type	Arabidopsis homolog	Arabidopsis homolog name	*curl* mutant allele
SL2.50ch09	6010739	G	A	Exon 6	*Solyc09g014380.2.1*	plus	W262*[g]	nonsense	*AT2G38120.1*	*AtAUX1*	*curl-2, curl-6*
SL2.50ch09	6009292	G	T	Intron.4	*Solyc09g014380.2.1*	plus	-	intron	*AT2G38120.1*	*AtAUX1*	*curl-1, curl-3*

[a] The location in the chromosome in the tomato genome
[b] Position of nucleotide substitution according to tomato genome sequence database, version SL2.50 (Sol Genomics Network)
[c] Tomato genome sequence reference according to the position in column [b]
[d] Alternative nucleotide sequence/ nucleotide substitution according to the position in column [b]
[e] Location of nucleotide substitution of the gene in column [f]
[f] Gene mutated according to Sol Genomic Network database
[g] * represents a stop codon

Table 6 Adaxial and abaxial pavement cell size the *curl* mutants in the curly part measured by a scanning electron microscope

Line	Pavement cell size (μm)		Abaxial/adaxial pavement cell size ratio
	Adaxial	Abaxial	
WT	43.36 ± 2.1	42.11 ± 3.4	0.97
curl-1	36.04 ± 1.8	57.83 ± 6.4**	1.59**
curl-2	36.90 ± 1.2	58.69 ± 4.1**	1.61**
curl-6	38.07 ± 1.8	60.18 ± 1.3**	1.66**

Line	Pavement cell number (cell)		Abaxial/adaxial pavement cell number ratio
	Adaxial	Abaxial	
WT	1317.3 ± 49.5	1110.6 ± 70.8	0.84
curl-1	1207.5 ± 80.6	1073.5 ± 65.2	0.89
curl-2	1389.2 ± 105.2	1173.9 ± 26.9	0.85
curl-6	1304.3 ± 73.6	1156.8 ± 59.6	0.89

Values are means ± SE (n=9). The asterisks represent statistically significant differences in means with equal variants based on Student's t-test (**P<0.01).
The cell feature was measured at the mature leaf stage when the leaves were completely turned to curly, precisely in the same regions on adaxial and abaxial surfaces.
The *curl* mutants showed a significantly larger abaxial/adaxial pavement cell size ratio compared to that of the wild-type (WT).

Legends to figures

Fig. 1 Leaf morphology of the WT 'Micro-Tom' and three alleles of the *curl* mutants.

(A-B) Mature leaf morphology of mature *curl* mutants in (A) adaxial and (B) abaxial view. The leaf images were captured from 2-month-old plants from the 5th leaflet. Scale bar: 2 cm. (C-D) Young leaf appearance of *curl* mutants. (C) adaxial and (D) abaxial view. The newly developed young leaves of the *curl* mutants were flat and indistinguishable from those of WT. Scale bar: 1 cm) (E) Representative of the curl mutant (*curl-1*) when grown in *in vitro* culture. Scale bar: 2 cm. The curly phenotype was not restored (F-G) Wild-type (F) and representative *curl* mutant (G, *curl-1*) grown under well-watered conditions in the greenhouse. Plant images were captured from 2-month-old plant. Scale bar: 1.5 cm.

Fig. 2 Adaxial and abaxial surfaces of young (upper panel) and mature (bottom panel) tomato leaflets.

(A) Adaxial (upper) surface of young tomato leaflets. (B) Abaxial (bottom) surface of young tomato leaflets. Young leaflets were detached from 1.5-month-old plants. (C) Adaxial (upper) surface of mature tomato leaflets. (D) Abaxial (bottom) surface of mature tomato leaflet. Mature leaflets were detached from the 5th leaflet of 2.5-month-old plants. Scale bar: upper panel, 3 cm; bottom panel, 2 cm.

Fig. 3 Partial chromosome mapping result of the *curl* mutant locus.

The *curl* locus was found to associate with the marker 14109-151 on chromosome 9 in the F_2 mapping population derived from the cross between *S. lycopersicum* cv. 'Ailsa Craig' x *S. lycopersicum* cv. 'Micro-Tom' *curl-2*. The marker information was obtained from the Kazusa DNA Research Institute AMF_2 database (http://marker.kazusa.or.jp/). No such association was observed in other chromosomes (Supplementary Table S3).

Fig. 4 Identification of *SlLAX1* (*Solyc09g01480.2*) as the most plausible candidate gene responsible for the *curl* phenotype.

Genome-wide allele frequency data were obtained by exome sequencing of BCF_2 bulked segregants that show the *curl* mutant phenotype. To narrow down candidate efficiently, four mapping populations derived from independent *curl* alleles (*curl-1, 2, 3, 6*) were constructed and subjected to exome sequencing. In all four mapping populations, a strong association was commonly observed for mutations within the *SlLAX1* (*Solyc09g01480.2*) gene, which is a homolog of the Arabidopsis *AUXIN RESISTANT1* (*AUX1*) transporter gene. Black boxes indicate exons, transparent boxes indicate UTRs, and lines between boxes indicate introns.

Fig. 5 Changes in protein amino acid sequence and *SlLAX1* gene expression in *curl* mutants.

(A, B) A partial alignment of *SlLAX1* cDNA sequence (A) or deduced protein amino acid sequence (B) among the tomato reference (SL2.50), wild-type Micro-Tom, *curl-2*, and *curl-6*. The mutation in *curl-2* and *curl-6* causes a premature stop codon, as shown by the red box (W262X). (C, D) A partial alignment of *SlLAX1* cDNA sequence (C) or deduced protein amino acid sequence (D) among the tomato reference (SL2.50), wild-type Micro-Tom, *curl-1*, and *curl-3*. cDNA sequences were obtained by dideoxy sequencing (A, C). (E) Donor and acceptor splicing sites in intron 4 of the wild-type, *curl-1*, and *curl-3* mutants. Square brackets indicate splicing sites. Double square brackets indicate alternative splicing site in the *curl-1* and *curl-3* mutants. The one-letter code indicates an amino acid. Uppercase indicates an exon, whereas lowercase indicates an intron sequence. The bold letter indicates a mutated sequence in intron 4 of the *curl-1* and *curl-3* mutants. The asterisk represents stop codon in the *curl-1*. (F) qRT-PCR analysis of *SlLAX1* gene expression. qRT-PCR primers were designed to target downstream of the stop codon mutation in exon 6. The asterisks represent statistically significant differences in the mean with equal variants compared to the wild-type (WT) based on Student's *t*-test ($^{**}P<0.01$). *SlActin* gene was used as an internal control. The expression level of the *curl-1*, *curl-2*, and *curl-6* mutants was relative to the wild-type (WT) expression.

Fig. 6 TILLING screening results and confirmation of the presence of curly leaf phenotype, cDNA and amino acid sequence alignment of the new mutant allele, TOMJPW601-1/*curl-7*.

(A) Polyacrylamide gel image of TILLING screening. The mutation in TOMJPW601-1/*curl*-7 is shown as an intense spot on the lanes both in IRD-700 (red circle) and IRD-800 (green circle). A single nucleotide change is shown on the sequence chromatogram (red arrowhead). (B) Whole-plant images of *curl-6* (left); a representative of the *curl* allele obtained using forward genetics; (middle and right) confirmation of the presence of curly leaves in the new selected allele, *curl-7*, in the M_3 generation. Plant images were captured from 2-month-old plants when the curly leaf phenotype progressed. Scale bar: 2 cm. (C) A partial alignment of *SlLAX1* cDNA sequence among the tomato reference (SL2.50), wild-type 'Micro-Tom', and TOMJPW601-1/*curl-7*. Nucleic acid substitution in the *curl-7* mutant is shown by a gray highlight. (D) Partial protein amino acid sequence alignment of *SlLAX*1 (*Solyc09g01480.2*) among the tomato reference (SL2.50), wild-type 'Micro-Tom', and TOMJPW601-1/*curl-7*. Mutation in *curl-7* led to the conversion of tryptophan to a premature stop codon. The wild-type (WT) produced a 411-a.a. product, whereas *curl-7* produced only a 185-a.a. product. The premature stop codon is indicated by a red box.

Fig. 7 Adaxial and abaxial pavement cell in the WT and the *curl* mutants at the curly part.

(A) The adaxial pavement cell size of WT and mutants was comparable Scale bar: 20 µm (B) The pavement cell size of all *curl* mutants in abaxial surface was significantly larger compared to that of wild-type. Scale bar: 10 µm. (C) The adaxial and abaxial sides of the curly part of leaf that were subjected to the scanning electron microscope experiment. Images were captured using a scanning electron microscope with 400x magnification at precisely in the curly part both in adaxial and abaxial surfaces.

Fig. 8 Relative expression of auxin-related genes which were reported to control leaf flatness, observed by qRT-PCR at young and mature leaf stages.

(A-E) Relative expression of gene at young leaf stage (A) *SlDof25* (B) *SlDof28* (C) *SlLCR* (D) *SlYUC1* (E) *SlPNH* (F) Adaxial specification gene *SlRev* (G-L) Relative expression of gene at mature leaf stage, when leaf completely turned to curly (G) *SlDof25* (H) *SlDof28* (I) *SlLCR* (J) *SlYUC1* (K) *SlPNH* (L) Adaxial specification gene *SlRev*. Values are means ± SE (n=3). The asterisks represent statistically significant differences in means with equal variants compared to the wild-type (WT) based on Student's t-test (*P<0.05, **P<0.01). *SlActin* gene was used as an internal control. The expression level of the *curl-1*, *curl-2*, and *curl-6* mutants was relative by the wild-type (WT) expression.

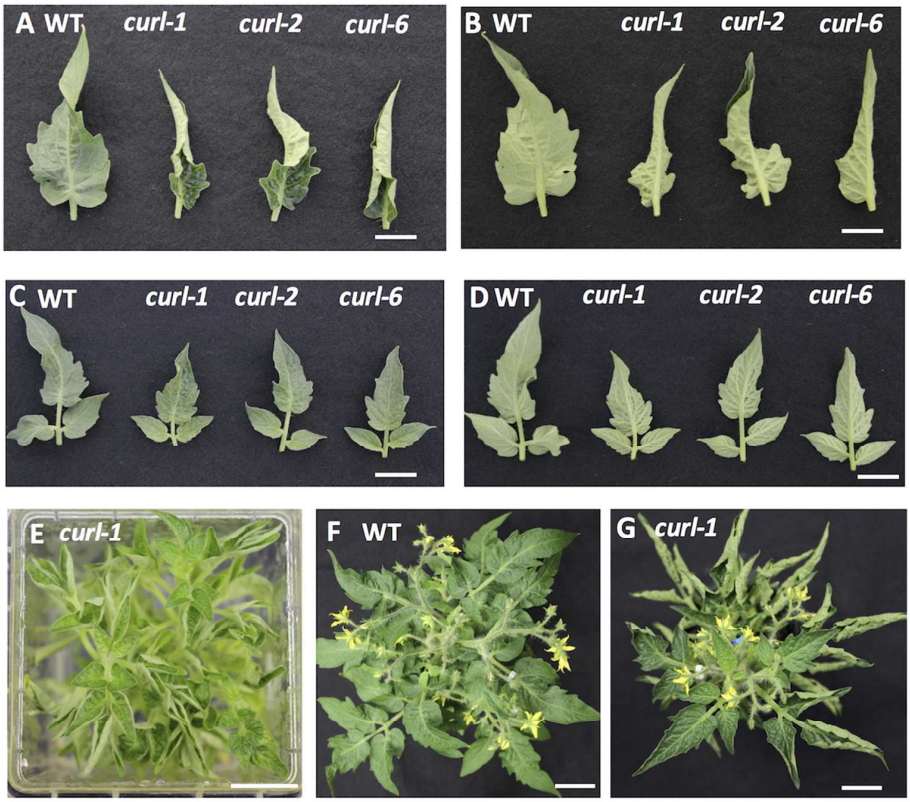

Fig. 1

99x88mm (300 x 300 DPI)

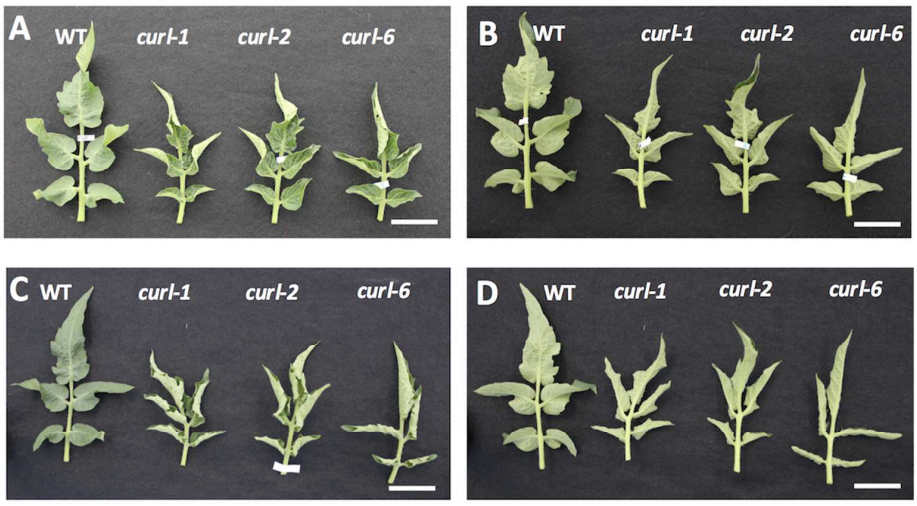

Fig. 2

99x56mm (300 x 300 DPI)

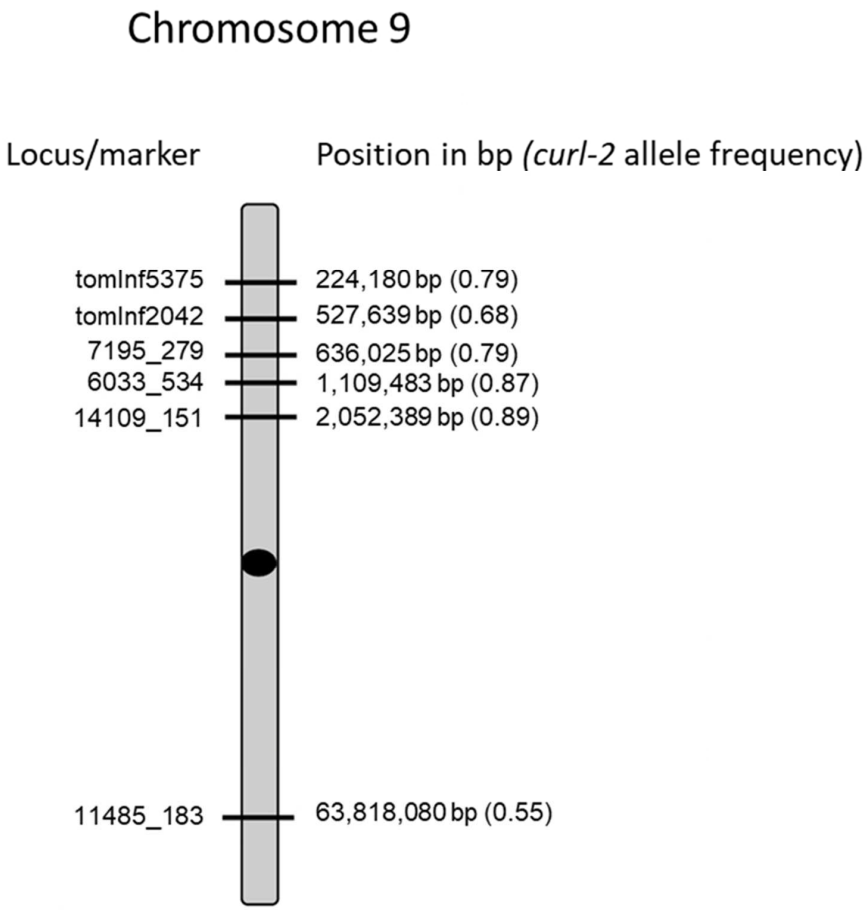

Fig. 3

80x85mm (300 x 300 DPI)

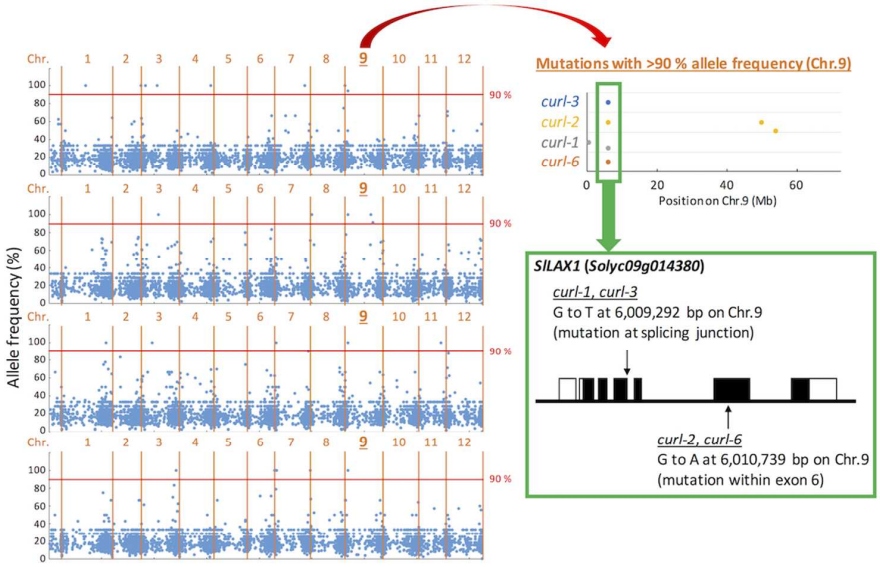

Fig. 4

99x69mm (300 x 300 DPI)

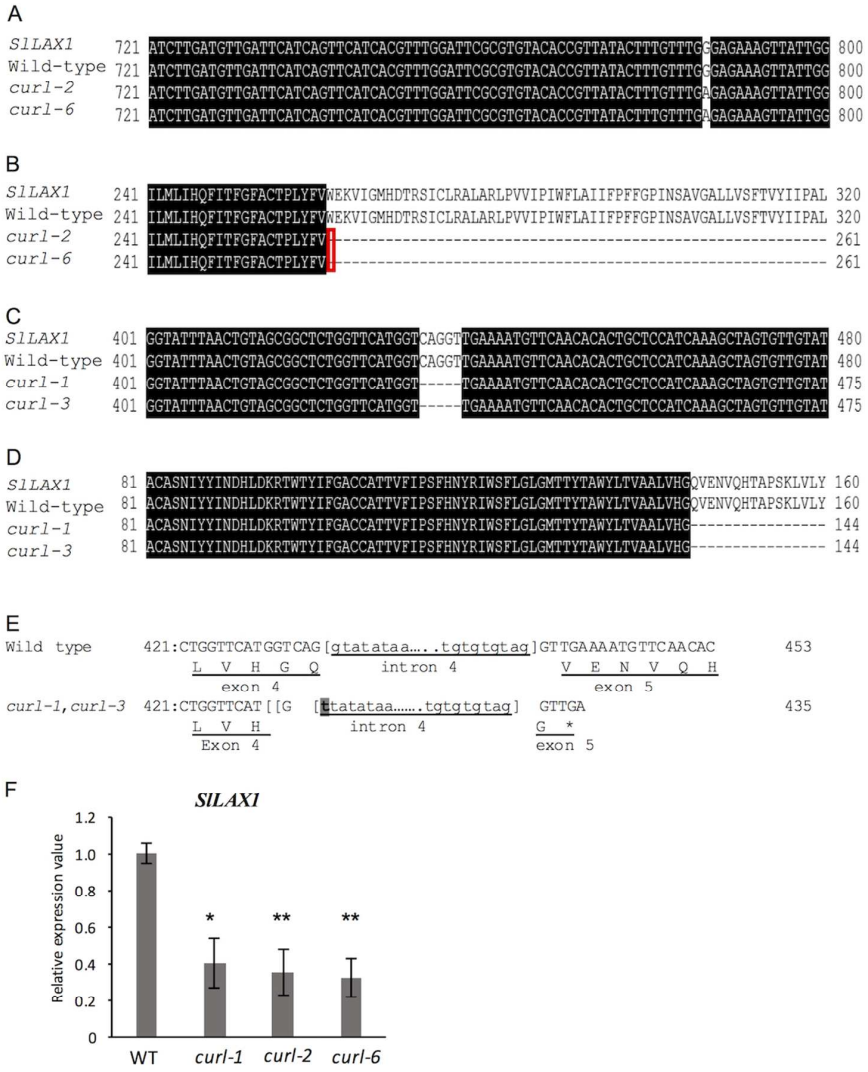

Fig. 5

99x122mm (300 x 300 DPI)

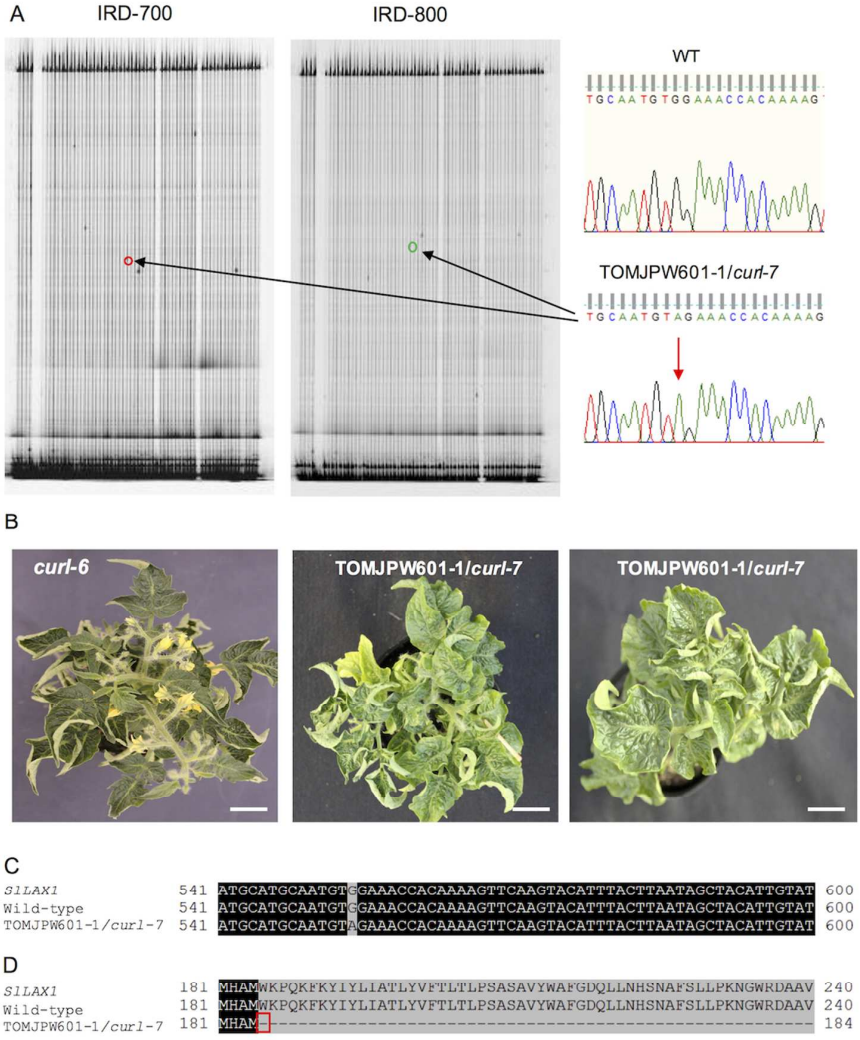

Fig. 6

99x121mm (300 x 300 DPI)

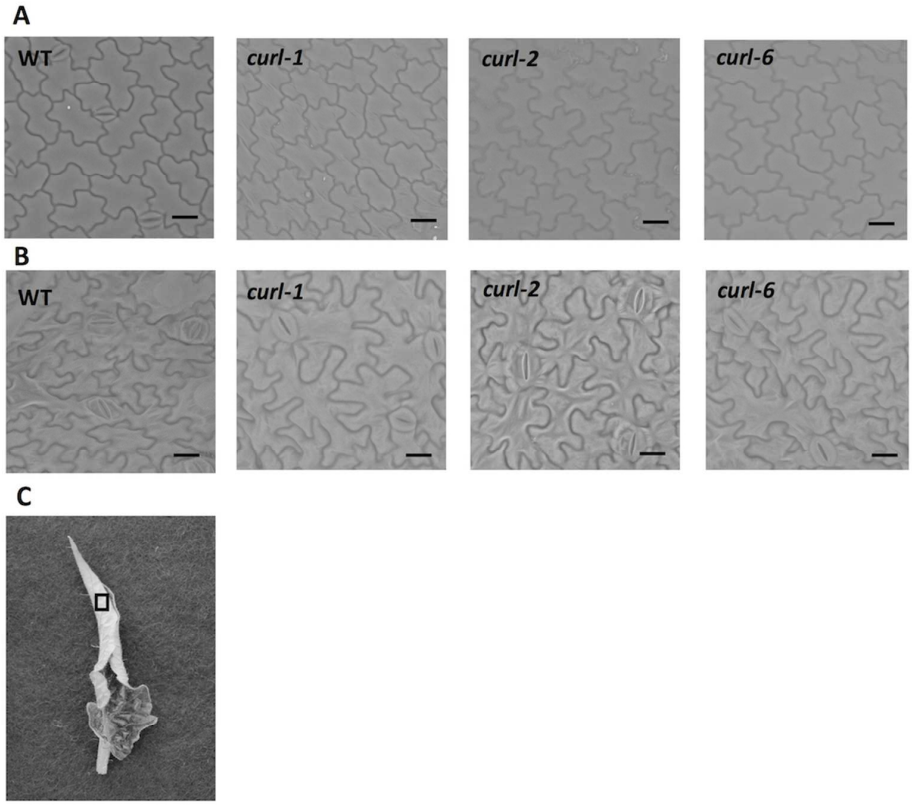

Fig. 7

99x88mm (300 x 300 DPI)

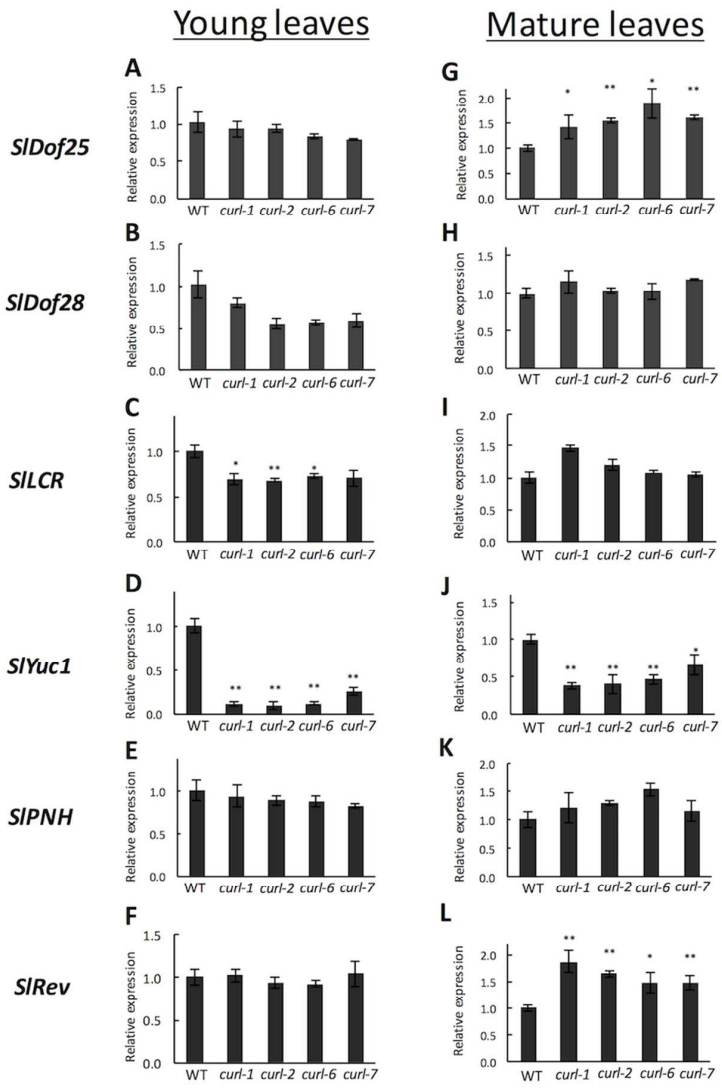

Fig. 8

80x113mm (300 x 300 DPI)